Computer Vision for Detection of Illegal Mining Barges in the Rio Madeira

Julian Lee[1*], **Eric Lin**[1*], **Maggie Wang**[1*] and **Sayak Maity**[1*]

[1] Harvard College
[*] Equal Contribution

{slee5, eric_lin, maggiewang, smaity}@college.harvard.edu

Abstract

In recent years, computer vision analysis of satellite imagery has been used to identify large ships in both offshore and inland settings, as well as to combat deforestation in the Amazon Forest. However, the presence of mining barges conducting ecologically destructive gold dredging operations in inland rivers remains a major problem relatively unaddressed by artificial intelligence. Challenges in this domain include the small size of the barges in question, their rapid movement patterns, and inconsistent satellite image availability, leading to high difficulty in detection. In our paper, we present three key contributions: (i) a self-curated medium-resolution satellite image dataset ($n = 296$) of small river watercraft, (ii) a temporal image differencing algorithm using radar data to detect watercraft movement under cloud coverage, and (iii) a convolutional neural network model trained using weighted cross-entropy loss that achieves 90.0% balanced accuracy and 100.0% TPR on a small held-out portion of our dataset. To the best of our knowledge, our work is the first application of artificial intelligence to identify small inland watercraft, and our dataset is also the first of its kind.

1 Introduction

Areas in the Amazon River Basin such as the state of Rôndonia in Brazil are rich in gold [1]. Gold prices have increased over 300% in the past two decades, and have recently gone over $1,700 per ounce. This has caused gold mining to be both lucrative and widespread.

Dredging of the Amazon River is generally harmful to the ecosystem. Gold mining operations have caused mercury contamination in the river, which negatively impacts local wildlife. Although there are occasional police patrols in the area, the Brazilian government's stance is that the large geographical region makes it too difficult to police the illegal miners. This serves as the motivation of our project as predicting illegal mining can narrow down search areas and accelerate policing.

Satellite imagery data currently does not exist for inland rivers and barges. Current solutions focus on massive ship classification. In addition, current solutions are ineffective because they don't have working relationships with local enforcement for feedback and explanation.

We solve the problem of being able to detect the presence of an illegal gold mining barge in the Amazon River based on satellite imagery. This will allow the World Wildlife Foundation (WWF) to better conduct research into the problem, and enable more targeted police enforcement against illegal mining.

Our main contributions are the following:

- We use spatial-temporal differencing of radar data to detect small barges in the Amazon river.
- We create the first-of-its-kind barge dataset [2] along with a custom CNN model to detect barges from optical data. In previous work, these datasets only had boats in ocean water far from land.
- We utilize both radar and optical data, as well as the MASATI dataset for transfer learning, to create novel a barge identification system that can be used for local enforcement. This includes both temporal differencing and deep learning models [1].

Figure 1: An example of a barge in the Amazon river. Gold mining in the river is harmful to the ecosystem because of the mercury contamination it produces.

[1] Please view our code at our GitHub Repo

2 Related Work

Advances in imagery and object detection models have led to increased research on using satellite imagery for watercraft identification. Current literature largely focuses on using either synthetic aperture radar (SAR) or optical remote sensing images for ship detection. However, these techniques are not generalizable to trickier environments, such as smaller watercraft in inland river areas.

SAR images have been preferred in past research due to their capabilities of seeing through clouds and independence from sunlight, making them work in all weather conditions at any time of the day. Previously, high-quality SAR images were hard to curate, leading to techniques working with simulated images [3]. An increase in the number of satellites capable of SAR imagery led to more widely available SAR datasets and more advanced models [4]. Then, ship detection was accelerated with the advent of deep learning [5]. Kang et al. showed in [6] how modifying the Faster R-CNN architecture with the constant false alarm rate (CFAR) algorithm led to increased accuracy for smaller-sized targets. This was improved further by [7] using YOLOv2 models.

Limitations on SAR image quality led to shortcomings in more complex marine areas with shores, islands, and uneven surfaces. To address this, optical remote sensing images, with much higher quality compared to SAR, were employed. Earlier algorithms using 2D object detection [8] were improved by threshold segmentation [9] and finally supplanted by the same Faster R-CNN models used for SAR imagery [10]. Unfortunately, optical imagery does lack the same benefits as SAR imagery in that clouds and night time dramatically degrade the use of images.

However, this previous work has all largely focused on ship detection in open seas or large river ports, which is strikingly different from the small barges and inland rivers the WWF and other conservation groups work with around the globe. Analysis of satellite imagery has previously been used to target illegal gold mining in the Amazon rainforest to curb deforestation [11]. Illegal sand, gravel, and gold mining [12] occur at alarming rates around the world, yet there is no known prior research in helping authorities detect these practices using image detection.

Our work addresses this problem by presenting novel datasets and solutions for identifying small parked barges in the river, rather than large ships in the open ocean or analyses of land-based operations. By using both SAR and optical imagery, we utilize the benefits of both approaches. In addition, our collaboration with the WWF was important in shaping the specifications for this project.

3 Data & Challenges

We encountered many challenges relating to the procurement of data. First and foremost, we had to curate our own training and testing datasets from satellite image databases, because existing datasets of satellite images containing watercraft are heavily focused on large cargo ships and not small inland barges. This already imposed a practical constraint on our dataset size, as due to time and labor constraints as well as the geographical sparsity of barges, the number of images that we could realistically source, process, and label was extremely limited.

In the process of data curation, we were further constrained by the competing considerations that our satellite image sources had to be high-resolution enough to display mining barges, which range from 50m to just 10m in length, but also available at low-cost for an unlimited length of time so that our solution would be sustainably usable by monitoring groups like the World Wildlife Fund and indigenous peoples. Moreover, we required a high temporal frequency of imaging in order to differentiate between moving watercraft, which are more likely to be innocuous, and watercraft parked in one location over multiple days, which are much more likely to be conducting illegal mining operations. Robustness to cloud coverage was a final major issue, as cloud coverage can render several consecutive days of images unusable for analysis.

Our proposed solution uses three different sources of data to cumulatively address all of these challenges. An overview of the approaches we used can be found in Figure 2.

3.1 Planet Labs Optical Data

Planet Labs is a commercial satellite image provider that provides images of 3m / px resolution using its PlanetScope satellites - we were able to access these images for free under its Education and Research program. This represented an appropriate balance of low cost, acceptable resolution, and daily revisit time to our Area of Interest (AOI).

Using our access to the Planet Labs database [13], we curated a dataset [2] of 296 square image tiles of the Madeira River in Rondônia State, ranging from 224x224px to approximately 300x300px. This dataset includes 100 samples manually labeled as ‘positive’ - meaning the tile contains a barge - and 196 samples labeled as ‘negative’. Because of the geographical sparsity of barges, downloading large swathes of river imagery and then labeling afterward was infeasible, as this would have led to a class imbalance skewed towards the negative by hundreds or thousands of times.

Instead, we manually searched through the image database for positive samples via visual inspection, individually downloading, square-cropping, and processing each one. We took the same approach for negative samples, which were considerably more abundant. For negative samples, we endeavored to proportionally represent in our dataset the wide range of non-boat-containing images which the model might encounter in the real world, including sediment deposits and clouds which could easily be mistaken for boats.

3.2 MASATI Pre-Training Data

The MASATI (MAritime SATellite Imagery) dataset [14] consists of optical images of maritime scenes, with image class divisions including with/without ships, and with/without coastline. This data is originally obtained from Microsoft® Bing Maps. The typical image in the dataset has a resolution of approximately 512x512 pixels.

Figure 3: Selected Positive Samples from Planet Labs Dataset

Figure 4: Selected Negative Samples from Planet Labs Dataset

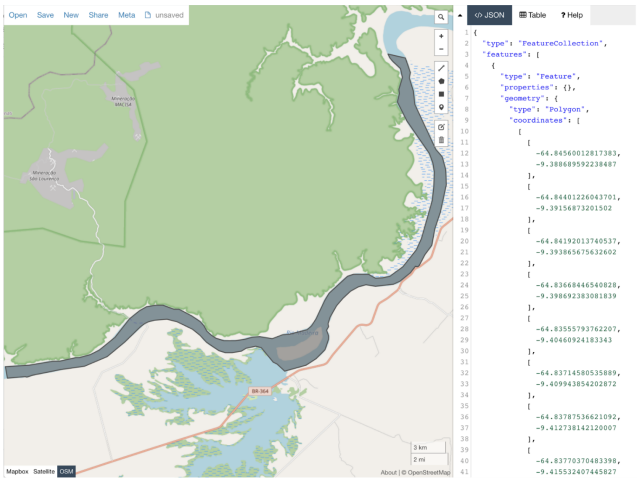

Figure 5: GeoJSON of selected Amazon River region used for Sentinel-1 radar data.

3.3 Sentinel-1 Radar Data

Sentinel-1 [15] is a constellation of two satellites launched by the European Space Agency. It collects radar data at a resolution of 10m / px, and the frequency of coverage is 3 days. The data is freely available via Sentinel Hub. Although the resolution of the radar data is lower than that of the Planet Labs optical data, radar data has some salient advantages as well. First, the data is not obscured by cloud coverage, which provides increased reliability. Second, radar data can also be collected at night, which is useful for this application because illegal gold mining barges can also operate at night.

We use a GeoJSON of the area of interest near Rio Madeira.

4 Evaluation

4.1 Radar Approaches

We use a single polarization (VV), which offers high contrast between the ships and water. We then mask the image using the GeoJSON shown in Figure 5, which allows us to find temporal differences between two images only in the river regions we are interested in, as shown in Figure 6c.

Using the masked radar image from two different dates, we take a temporal difference between the recent date we are interested in and a later date. The temporal difference allows ships and barges in the more recent date to have a higher pixel value. We deploy a binary threshold in OpenCV to extract only the pixels with high value where the ships and barges

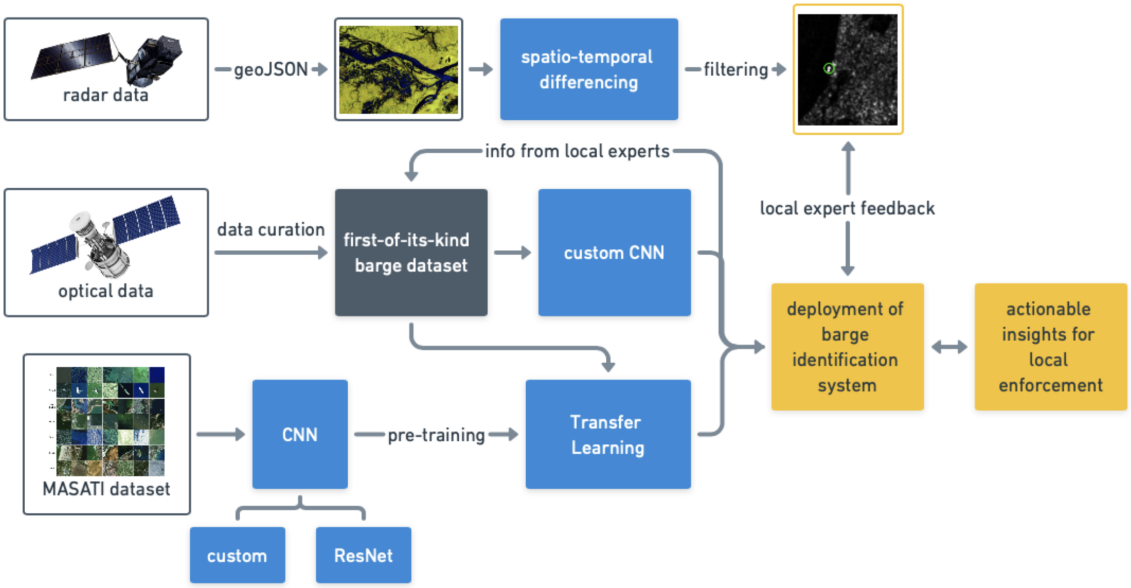

Figure 2: Overview of our approach.

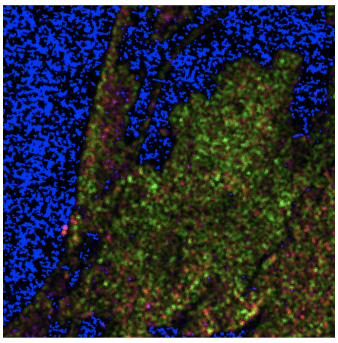

(a) The full Sentinel-1 image with four bands.

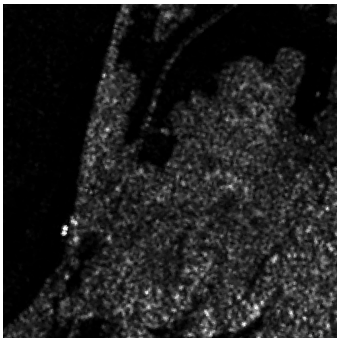

(b) Sentinel-1 radar image with a single band (VV).

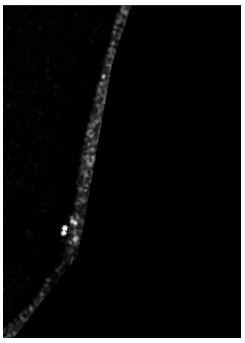

(c) Sentinel-1 radar image (VV) with masking using the GeoJSON of desired locations of the Amazon River.

Figure 6: The Sentinel-1 data processing pipeline, where we start from a single image band and use a GeoJSON mask to focus only on regions of interest.

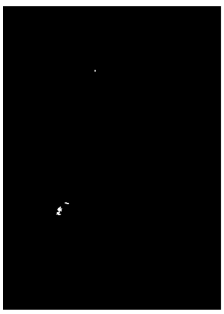

(a) We take a temporal image difference between the recent time period we are interested in and an earlier time period. This gives us higher pixel values where there are emerging objects of interest in the recent time period. We then use a binary threshold to remove extraneous values.

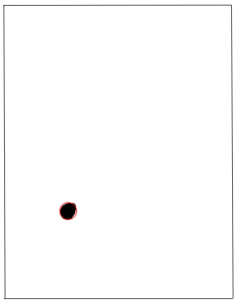

(b) We use a Gaussian blur along with a simple blob detector in OpenCV to filter the objects of interest by area. This allows us to filter for barges and ships in the river.

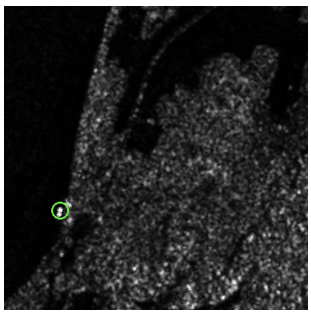

(c) After we find the keypoint location and radius of the blob, we overlay the final detection point on the initial Sentinel radar image to verify the location of the ship or barge.

Figure 7: Temporal difference and filtering steps in the Sentinel-1 pipeline.

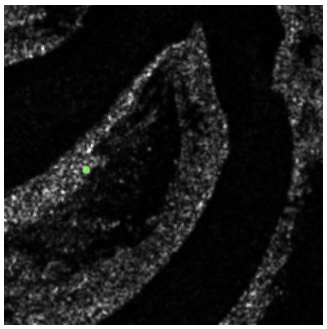

(a) False positive found by the spatial-temporal difference method. This false positive occurred because the GeoJSON does not completely cut out where the land is, and we occasionally get spurious detections on land.

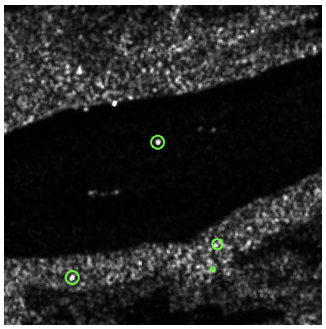

(b) The circle in the middle created by the spatial-temporal difference method correctly identifies a barge. The two circles near the bottom of the image are spurious detections due to an imperfect GeoJSON outline of the Amazon river.

Figure 8: False positives found by the Sentinel-1 radar spatial-temporal difference technique. We designed our system to be more lenient towards false positives and strict towards false negatives, since we will have a person verifying the detection output of our system.

are most likely to be.

We then use a Gaussian blur and blob detector to filter the detections by area, as shown in Figure 7a. We get the keypoint location and radius from the blob and draw the keypoint on the initial radar image, as shown in Figure 7c.

We found that there were no false negatives found in the time interval of interest, but we saw multiple false positives due to an imperfect GeoJSON outline of the river. These false positives can be seen in Figure 8. Since the WWF teams in Brazil will be verifying the final output of our system, we designed our system to be more lenient towards false positives and strict towards false negatives.

4.2 Optical Approaches

In order to work with the small size of our curated dataset, we compared a transfer learning approach to a from-scratch training approach, and surprisingly found the from-scratch training, with certain strategic modifications, to perform better than the transfer learning approach by up to 6.5%. In all experiments, we used 5-fold cross-validation on the Planet Labs curated dataset, with one fold of 60 images being held out until after model selection in order to estimate generalization capacity, and the other four folds of 59 images each being used once as a validation fold for model and hyperparameter selection.

Although training from-scratch at times outperformed the transfer learning approach for certain w_{pos} thresholds, pretraining did improve stabilization of model performance, as seen in Figure 10. The 6.5% improvement sometimes exhibited by training from-scratch only accounts for a difference of 16 more images labeled correctly across the 5-fold cross validation in aggregate. Moreover, as w_{pos} is increased, we see a more stable and consistent increase in positive accuracy for the pretrained model.

The average of all four validation accuracies was used to evaluate hyperparameter and model settings, an approach which was especially necessary given our small dataset - we found that single train and validation cycles had extremely high variance and were very unstable depending on the train / val / test split used. In order to simulate an inflation of the dataset size, training images were augmented with random horizontal and vertical flips, a random 224x224 crop, and standard color jitters.

Weighted Cross-Entropy Loss

One of the major techniques we incorporated in order to adapt models to this domain was weighted cross-entropy loss. Weighted cross-entropy loss was originally developed to handle significant class imbalances in datasets, preventing models from neglecting small classes by disproportionately penalizing the misclassification of samples from underrepresented classes during training. In the binary classification case, weighted cross entropy loss is parameterized by a single hyperparameter, w_{pos}, indicating the loss incurred by the misclassification of a positive sample proportionate to the loss incurred by an equally confident misclassification of a negative sample. This is expressed as

$$L(y, p) = -(w_{pos} y \log(p) + (1 - y) \log(1 - p))$$

where p is the probability assigned to the positive class by the model, usually derived through applying the softmax function over the model's output vector. Standard cross-entropy loss is equivalent to the case where $w_{pos} = 1$; if $w_{pos} > 1$, we consider correct classification of positive samples to be more important than correct classification of negative samples, and if $w_{pos} < 1$, the opposite holds true.

Weighted cross-entropy was especially important in our modeling because of the low penalty incurred by false positives in the real world application of our research. In the human-in-the-loop system that we envision, a human user could easily verify and dismiss tens of false positives in a matter of seconds, while a false negative would represent a significant missed opportunity to prevent illegal mining. While a strong balanced accuracy remained an objective, a high True Positive Rate (TPR) is more important to human decision-makers than a high True Negative Rate (TNR), and so a large part of our experimentation revolved around tuning the w_{pos} hyperparameter to determine which setting best matched this goal.

Custom CNN

We first trained a custom CNN architecture on our curated Planet Lab dataset. With RGB input square images of 3x224x224, the sequential model consisted of a convolutional block with 3 convolutional kernels of size 32x32, followed by 7 convolutional blocks of 3 kernels of size 128x128. The final layer is a fully-connected layer taking the outputs of the convolutional blocks and outputting a binary label. We designed this custom CNN to be smaller and more lightweight, since we anticipated that without pre-training on MASATI, the taks of learning binary classification of barge vs. no barge wouldn't need as deep of a model. In Table 1, we can see that the custom model achieved moderate 5-fold validation accuracy with $w_pos = 1.5$.

	balanced acc.	TPR	TNR
Custom, no pre-training	0.73	0.71	0.78
ResNet18, no pre-training	0.83	0.82	0.84
ResNet18, pre-trained	0.77	0.65	0.88

Table 1: Averaged 5-fold cross validation accuracies for custom and ResNet18 models with no pre-training ($w_{pos} = 1.5$) and pre-trained ResNet18 ($w_{pos} = 2.0$)

.

Hyperparameter Optimization

In Figures 9 & 10, we compare the effects of tuning w_{pos} for a ResNet-18 initialized randomly and with weights learned from pre-training on the MASATI dataset. We observe that tuning w_{pos} has a more significant positive effect on the randomly initialized than on the pre-trained network. With standard cross-entropy loss ($w_{pos} = 1.0$), the transfer learning approach significantly outperforms the from-scratch training, with a 75.5% vs. a 67.5% balanced accuracy. Notably, the from-scratch training with $w_{pos} = 1.0$ had a TPR of just 52%, which was equivalent to random guessing, compared to the 80% achieved by the pre-trained network.

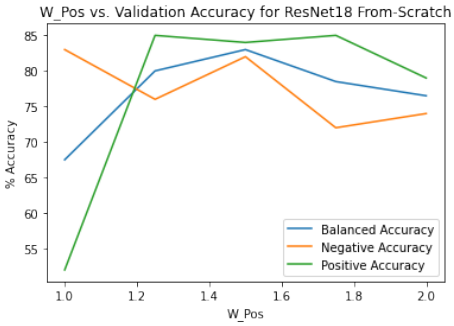

Figure 9: w_{pos} vs. validation accuracy for ResNet-18 from scratch

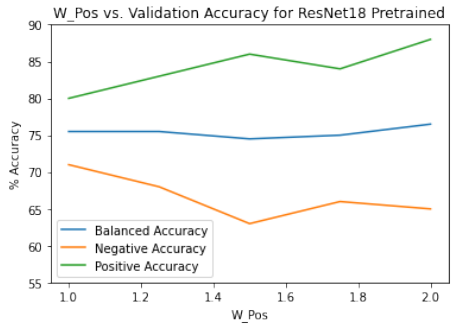

Figure 10: w_{pos} vs. validation accuracy for ResNet-18 pretrained

Increasing w_{pos} appears to have no effect on balanced accuracy for the pretrained ResNet18 - as expected, we see incremental gains in TPR as w_{pos} increases, but in order to achieve these gains the model makes similarly sized sacrifices in TNR, so that balanced accuracy is almost unchanged. On the from-scratch network, however, we observe that the gains in TPR as w_{pos} increases are significant enough to outweigh the sacrifice in TNR - in particular, the TPR jumps by over 40% when w_{pos} is tuned from 1.0 to 1.25. We chose $w_{pos} = 1.5$ on the from-scratch model, which trained to 84% validation TPR and 82% validation TNR as our final setting, retrain over all four train/validation folds, and test on the holdout fold to estimate generalization capacity. The testing yielded a TPR of 100% and a TNR of 80%, an impressive and surprising result which suggests that this particular testing fold contained an especially 'easy' set of samples.

4.3 Proposed Integration of Radar and Optical Approaches

In practice, we propose to integrate the temporal differencing and deep learning models by regularly checking the Planet Labs API for cloud-free images over our AOI. After running the images through our optical machine learning pipeline and identifying candidate tiles containing small watercraft, we can then use the georeferencing of the tile to determine whether the craft was located within the Protected Areas designated by the Brazilian government and the government of Rondônia. Finally, we would utilize our temporal differencing radar approach to verify the presence of the barge, guarding against the high false positive rate, and determine the length of time that it has been stationary. Optically identified barges that were pictured in a Protected Area and were shown to be stationary over a period of multiple days would then be flagged to partners at the World Wildlife Fund and within indigenous groups for in-person intervention. For real-world usage by the WWF researchers and local police, these tools will be built into a mobile app, since that is the most common and accessible option.

5 Ethics & Broader Impact

With the creation of new technology tools, it is also important to consider the ethics and broader impact of using the technology. First, we would want to ensure that the local governments are using the tools as we intended. Misuse in general can be mitigated through user training when onboarding to the platform. For concerns regarding surveillance, a geofence can be set in the app to only reveal satellite imagery in the relevant river areas and protected regions. In addition, the satellite imagery itself, having a maximum resolution of 3m / px, is not sufficiently high resolution to pose a threat to individual privacy. Another ethical concern is how it will affect the livelihood of the gold miners. Families with small children live and work on these barges and depend on gold mining for income. The disruption of their lives is a relevant social cost that should be considered as this technology is further refined and deployed. Some of the broader impacts of this project include a positive environmental impact. Less illegal gold mining in the Amazon River will translate into better ecosystem health and less mercury contamination for wildlife. Notably, since humans consume fish from the Amazon river, successful reduction of illegal gold mining would ultimately improve human health.

6 Conclusions and Future Work

Through this research, we have made two primary contributions. The first is that we have created a novel dataset for barge detection in rivers. The task is distinctly more challenging than previous work done on ship detection due to constraints including low resolution and small size of the barges. In addition, ambiguity in detection arises if barges are close to the shore, and if other visual artifacts are present. The second primary contribution is proving the feasibility of using computer vision techniques and convolutional neural networks to successfully detect barges with a sufficiently high level of accuracy for field use.

In the future, this model could be improved through training on a larger dataset. Other techniques such as constrative learning or few-shot detection may increase accuracy with limited datasets. Work is also greatly needed in addressing similar illegal sand and gravel mining around the world. We would like to see more research conducted with local experts as a human in the loop in these AI detection systems.

7 Acknowledgements

Thank you to Prof. Milind Tambe, WWF Senior Analyst Felipe Spina Avino, and the teaching staff of Harvard CS 288.

References

[1] J. J. Swenson, C. E. Carter, J.-C. Domec, and C. I. Delgado, "Gold mining in the peruvian amazon: Global prices, deforestation, and mercury imports," *PLOS ONE*, vol. 6, no. 4, pp. 1–7, 04 2011. [Online]. Available: https://doi.org/10.1371/journal.pone.0018875

[2] E. L. M. W. Julian Lee, Sayak Maity, "Amazon Barge Detection Dataset," 2021. [Online]. Available: https://github.com/sayakmaity/planet-data-288

[3] G. Margarit, J. J. Mallorqui, J. M. Rius, and J. Sanz-Marcos, "On the usage of grecosar, an orbital polarimetric sar simulator of complex targets, to vessel classification studies," *IEEE Transactions on Geoscience and Remote Sensing*, vol. 44, no. 12, pp. 3517–3526, 2006.

[4] M. Tello, C. López-Martínez, and J. J. Mallorqui, "A novel algorithm for ship detection in sar imagery based on the wavelet transform," *IEEE Geoscience and remote sensing letters*, vol. 2, no. 2, pp. 201–205, 2005.

[5] M. Ma, J. Chen, W. Liu, and W. Yang, "Ship classification and detection based on cnn using gf-3 sar images," *Remote Sensing*, vol. 10, no. 12, p. 2043, 2018.

[6] M. Kang, X. Leng, Z. Lin, and K. Ji, "A modified faster r-cnn based on cfar algorithm for sar ship detection," in *2017 International Workshop on Remote Sensing with Intelligent Processing (RSIP)*. IEEE, 2017, pp. 1–4.

[7] Y.-L. Chang, A. Anagaw, L. Chang, Y. C. Wang, C.-Y. Hsiao, and W.-H. Lee, "Ship detection based on yolov2 for sar imagery," *Remote Sensing*, vol. 11, no. 7, p. 786, 2019.

[8] S. Li, Z. Zhou, B. Wang, and F. Wu, "A novel inshore ship detection via ship head classification and body boundary determination," *IEEE geoscience and remote sensing letters*, vol. 13, no. 12, pp. 1920–1924, 2016.

[9] F. Yang, Q. Xu, and B. Li, "Ship detection from optical satellite images based on saliency segmentation and structure-lbp feature," *IEEE Geoscience and Remote Sensing Letters*, vol. 14, no. 5, pp. 602–606, 2017.

[10] S. Zhang, R. Wu, K. Xu, J. Wang, and W. Sun, "R-cnn-based ship detection from high resolution remote sensing imagery," *Remote Sensing*, vol. 11, no. 6, p. 631, 2019.

[11] D. O. Fuller, "Tropical forest monitoring and remote sensing: A new era of transparency in forest governance?" *Singapore Journal of Tropical Geography*, vol. 27, no. 1, pp. 15–29, 2006.

[12] M. A. Ashraf, M. J. Maah, I. Yusoff, A. Wajid, and K. Mahmood, "Sand mining effects, causes and concerns: A case study from bestari jaya, selangor, peninsular malaysia," *Scientific Research and Essays*, vol. 6, no. 6, pp. 1216–1231, 2011.

[13] P. Team, "Planet Application Program Interface: In Space for Life on Earth," Planet, 2017–. [Online]. Available: https://api.planet.com

[14] A. P. Antonio-Javier Gallego and P. Gil, "Automatic ship classification from optical aerial images with convolutional neural networks," *Remote Sensing*, vol. 10, no. 4, 2018.

[15] "Modified Copernicus Sentinel data/Sentinel Hub," European Space Agency, 2021. [Online]. Available: https://www.sentinel-hub.com/